Nucleophosmin interaction with APE1: Insights into DNA repair regulation.

David J. López, Ander de Blas, Mikel Hurtado[1], Mikel García-Alija[2], Jon Mentxaka, Igor de la Arada, María A. Urbaneja, Marián Alonso-Mariño, Sonia Bañuelos*

Biofisika Institute (UPV/EHU, CSIC) and Department of Biochemistry and Molecular Biology, University of the Basque Country (UPV/EHU), Leioa, Spain.

Present addresses: [1]NEIKER-Basque Institute of Agricultural Research and Development, c/ Berreaga 1, E-48160 Derio, Spain. [2]CIC bioGUNE-, E-48160 Derio, Spain.

Abbreviations: AML: acute myeloid leukemia; APE1: apurinic apyrimidinic endonuclease 1; BER: Base excision repair; CD: circular dichroism; DDR: DNA damage repair; DSB: double strand break; FT-IR: Fourier transform infrared spectroscopy; IR: ionizing radiation; ITC: isothermal titration calorimetry; NPM1: nucleophosmin; PA: polyacrylamide; PAGE: polyacrylamide gel electrophoresis; THF: tetrahydrofurane.

*Corresponding author at: Biofisika Institute, University of the Basque Country, Barrio Sarriena s/n, E-48940 Leioa, Spain. E-mail address: sonia.banuelos@ehu.es

Abstract

Nucleophosmin (NPM1), an abundant, nucleolar protein with multiple functions affecting cell homeostasis, has also been recently involved in DNA damage repair. The roles of NPM1 in different repair pathways remain however to be elucidated. NPM1 has been described to interact with APE1 (apurinic apyrimidinic endonuclease 1), a key enzyme of the base excision repair (BER) pathway, which could reflect a direct participation of NPM1 in this route. To gain insight into the possible role(s) of NPM1 in BER, we have explored the interplay between the subnuclear localization of both APE1 and NPM1, the *in vitro* interaction they establish, the effect of binding to abasic DNA on APE1 conformation, and the modulation by NPM1 of APE1 binding and catalysis on DNA. We have found that, upon oxidative damage, NPM1 is released from nucleoli and locates on patches throughout the chromatin, perhaps co-localizing with APE1, and that this traffic could be mediated by phosphorylation of NPM1 on T199. NPM1 and APE1 form a complex *in vitro*, involving, apart from the core domain, at least part of the linker region of NPM1, whereas the C-terminal domain is dispensable for binding, which explains that an AML leukemia-related NPM1 mutant with an unfolded C-terminal domain can bind APE1. APE1 interaction with abasic DNA stabilizes APE1 structure, as based on thermal unfolding. Moreover, our data suggest that NPM1, maybe by keeping APE1 in an "open" conformation, favours specific recognition of abasic sites on DNA, competing with off-target associations. Therefore, NPM1 might participate in BER favouring APE1 target selection as well as turnover from incised abasic DNA.

Keywords: APE1, NPM1, nucleophosmin, BER, base excision repair, protein-protein interaction.

Introduction

Nucleolus, beyond its canonical ribosome assembly function, is being increasingly recognized as a key hub in coordinating progression of the cell cycle and responses to cellular perturbations, such as damage to DNA (Boisvert et al., 2007; Emmott & Hiscox, 2009; Antoniali et al., 2014; Ogawa & Baserga, 2017). Upon sensing different types of stresses, the localization of several nucleolar components is modulated and their involvement in repair tasks orchestrated from this membrane-less organelle (Scott & Oeffinger 2016; Antoniali et al., 2014). Nucleophosmin (NPM1) is one of the nucleolar proteins that seem to be involved in DNA damage repair (DDR) mechanisms. NPM1 is homopentameric and consists of multiple domains: an N-terminal compact, β-structured core domain, responsible for oligomerization (Lee et al., 2007), is connected by long, flexible linkers, to small, helical, C-terminal domains (Grummitt et al., 2008). Although normally enriched in nucleoli, NPM1 continuously shuttles between cytoplasm, nucleoplasm and nucleolus (Lindström, 2011). NPM1 shuttling is mediated by transport receptors of the karyopherin family (importin α/β, exportin CRM1) (Lindström, 2011; Arregi et al., 2015), whereas nucleolar accumulation probably depends on its affinity for G-rich DNA or RNA sequences adopting special structures known as G-quadruplexes (Bañuelos et al., 2013; Chiarella et al, 2013). NPM1 is in charge of multiple functions related to cell homeostasis, including biogenesis and export of ribosomes (Maggi et al., 2008), control of centrosome duplication (Wang et al., 2005), regulation of the stability of tumour suppressors such as p53 (Colombo et al 2002) and Arf (Colombo et al., 2005), and cell response to stress. Recent experimental evidence points to NPM1 as a key factor directly participating in DNA damage repair (DDR) pathways, although its role in these mechanisms remains to be established (Scott & Oeffinger 2016; Box et al., 2016; Koike et al., 2010; Moore et al., 2013; Ziv et al., 2014; Guillonneau et al., 2016; Yang et al., 2016).

Regarding NPM1 activity in the context of stress response, it was found associated with chromatin upon induction of double strand breaks (DSBs) with ionizing radiation (IR) or etoposide (Lee et al., 2005). The putative changes in subnuclear localization of NPM1 upon DSBs and its participation in the management of these lesions seem to be regulated by phopshorylation. T199-phosphorylated NPM1, which locates outside the nucleoli, is recruited to DSBs repair sites (*foci*) in response to IR (Koike et al., 2010). Moreover, NPM1 undergoes nucleoplasmic translocation upon different genotoxic

insults, such as oxidative stress, UV, cisplatin, etc. (Colombo et al., 2011; Scott & Oeffinger 2016; Yang et al., 2016) and, apart from DSBs repair, it has been implicated in yet further DNA repair pathways, namely translesion synthesis (TLS) (Ziv et al., 2014) and base excision repair (BER) (Vascotto et al., 2009; Vascotto et al., 2014).

NPM1 has been described to interact with APE1 (apurinic apyrimidinic endonuclease 1) (Vascotto et al., 2009), a key enzyme of the BER pathway, aimed to repair DNA damage caused by oxidizing or alkylating agents, including chemotherapeutic drugs (Almeida & Sobol, 2007; Krokan & Bjoras, 2013; Parsons & Dianov, 2013). APE1 specifically recognizes abasic sites in DNA and hydrolyzes the phosphodiester bond 5´of the abasic sugar (Freudenthal et al., 2015), generated after removal of a modified / damaged base by a specific glycosidase, or by spontaneous depurination (Li and Wilson, 2014). Afterwards, a polymerase restores the lacking nucleotide using the complementary strand as template, and the phosphodiester link is re-formed by a ligase. APE1 performs additional functions in the context of DNA repair (being able to correct "non productive" ends of DNA strands in repair intermediates) and, probably, in RNA management (as an "RNA quality control") (Antoniali et al., 2014). Besides its roles in DDR, APE1 acts as a redox coactivator of different transcription factors such as p53 and NF-κB. APE1 catalytic cycle on DNA has been described in structural detail (Mol et al., 2000; Freudenthal et al., 2015); however, the mechanisms regulating APE1 functionality are largely unknown.

NPM1 might have a role in BER repair, modulating the localization of APE1 (Vascotto et al., 2014). In the absence of DNA damage, APE1 locates through nucleoplasm and is enriched in nucleoli, which is probably mediated by its interaction with NPM1 through a flexible, N-terminal region of APE1. This region seems to also play a regulatory role in APE1 binding to DNA (Fantini et al., 2010; Vascotto et al., 2014). Furthermore, acetylation of lysine residues in this segment might modulate the interaction with NPM1 and thus APE1 nucleolar localization (Lirussi et al., 2012). The fact that, as mentioned, NPM1 itself may transit to the nucleoplasm depending on stress conditions and its own posttranslational modifications adds further complexity to the regulation of NPM1 and APE1 dynamics. A pool of APE1 seems to locate also in mitochondria, and could take part in the repair of oxidized DNA in this organelle (Li & Wilson, 2014). On the other hand, NPM1 participation in multiple, mechanistically different repair pathways might be also based on its chromatin remodelling (histone chaperoning)

capacities (Okuwaki et al., 2001). A further, as yet unexplored possibility is that NPM1 takes part directly in the BER enzymatic machinery. Indeed, NPM1 seems to slightly stimulate APE1 incision activity on abasic DNA *in vitro* (Vascotto et al., 2009). A direct involvement of NPM1 in repair tasks remains however to be confirmed, and the underlying mechanism deciphered.

DNA repair machineries are valuable targets in cancer, as long as interfering with their functioning can enhance the efficiency of antineoplasic therapies (Pilié et al., 2018). In this sense, APE1 is considered a target for chemosensitization and radiosensitization (Wilson & Simeonov, 2010; Li & Wilson, 2014). On the other hand, NPM1 is regarded as an oncoprotein, being deregulated (overexpressed, mutated and/or aberrantly located) in several types of human cancer (Grisendi et al., 2006). In particular, it is mutated, misfolded, and partly accumulated in the cytoplasm of tumour cells in a subtype of acute myeloid leukemia (AML) (Falini et al., 2005; Federici & Falini, 2013). NPM1 binds many ligands, so that when aberrantly located as in AML, might induce subsequent mislocalization of some of these partners. Indeed, it has been described that APE1 (Vascotto et al., 2014), amongst other proteins, may be, as a result, dislocated to cytoplasm in AML, an alteration perhaps related with triggering of the disease.

To better understand the role of NPM1 in DNA repair, as well as the pathological consequences of its mislocalization, we have explored the subnuclear dynamics of NPM1 and APE1 under stress conditions. In addition, we have characterized the interaction between both proteins and the effects of oncogenic mutations of NPM1 on the binding properties. Finally, we have evaluated the consequences of DNA binding on APE1 conformation, and the effect of NPM1 on APE1 binding to abasic DNA. Altogether, our results suggest a mechanism for regulation of APE1 activity by NPM1 and shed light on the putative role of APE1:NPM1 interaction in BER repair.

1. Material and methods.

1.1. Cell culture, transfection, treatment, imaging and immunoblotting.

The clone of human APE1 fused to EGFP was kindly provided by Dr. Izumi (Jackson et al, 2005). The gene was subcloned fused to C-terminal mCherry, between XhoI and SmaI sites of vector pCRY2PHR-mCherryN1, a gift from Chandra Tucker (Kennedy et

al., 2010). Human HeLa and HEK293T cells (DSMZ collection) were grown in Dulbecco's modified Eagle's medium, supplemented with 10% fetal bovine serum, 100 units/mL penicillin and 100 μg/mL streptomycin (all from Invitrogen). Transfections of cells, seeded onto sterile glass coverslips in 12-well trays the previous day, were carried out with XtremeGENE 9 (Roche) following the manufacturer's protocol.
Induction of oxidative damage and extraction of soluble proteins were done following a previously described protocol (Campalans et al., 2013). The next day after transfection, cells were treated with 0 – 300 mM $KBrO_3$ in PBS for 30 min at 37ºC, and afterwards grown for 3 h longer in fresh medium, in order to "recover". Then, prior to fixation with 3.7% formaldehyde in PBS for 30 min, cells were washed with 10mM PIPES pH 6.8, 100mM NaCl, 300mM glucose, 3mM $MgCl_2$, 0.5% Triton X-100 and a cocktail of protease inhibitors (Roche) (CSK-buffer, Campalans et al., 2013), to extract soluble proteins. Other treatments were done with 0.5 and 5 mM H_2O_2 (Sigma) for 30 min, 5 μg/mL neocarzinostatin (Sigma) for 4 h or 0.5 μg/mL nocodazole (Sigma) for 24 h.

For fluorescence immunostaining, fixed cells were further permeabilized with 0.2% Triton X-100 in PBS for 10 min, and incubated for 1 h in blocking solution (3% BSA in PBS). Endogenous NPM1 was detected with mouse anti-B23 (Santa Cruz Biotechnology FC82291, dilution 1:800 in blocking solution), and NPM1 phosphorylated at Thr199 with rabbit anti-NPM1p199 (Abcam EP1857Y, dilution 1:150). The secondary antibodies were Alexa Fluor 594 anti-mouse (Invitrogen A11005, dilution 1:400) and Alexa Fluor 594 anti-rabbit (Invitrogen A11012, dilution 1:400). Washing between the different steps was carried out with PBS. Cells were finally mounted on to microscope slides using Vectashield containing DAPI (Vector Laboratories). Cell imaging was performed with the support of SGIker Service (University of the Basque Country UPV/EHU). Routine images were taken with Zeiss Axioscope or Axio Observer Apotome 2 microscope. High resolution images (Fig. 1) were acquired in a Zeiss LSM880 with a 63x lens (Plan Apochromat, 1.4 NA), using the Fast Airyscan superresolution mode

Two days later, after the different treatments, they were gently washed with cold PBS, scraped on ice and resuspended in 50 μL of lysis buffer (Pierce) supplemented with a cocktail of inhibitors (Roche). Following lysis for 30 min and centrifugation, samples were loaded in a 12.5% PAGE gel and then transferred to a nitrocellulose membrane (GE Healthcare) in a wet apparatus (Bio-Rad). Then, the membrane was blocked with

5% (w/v) non-fat dry milk powder in TBS-T and incubated with the same primary antibodies (anti-NPM1, diluted 1:800 in blocking solution, and anti- NPM1p199, diluted 1:2500) as for immunostaining. As controls of loaded amount, anti- tubulin (Sigma Aldrich, T9026, dilution 1:5000) and anti-GAPDH (Santa Cruz Biotechnology, sc-25778, dilution 1:2000) were used. After washing steps with TBS-T, the membrane was incubated with the corresponding anti-mouse and anti-rabbit HRP- conjugated antibodies and finally detection was made with the Luminata Forte Western HRP Substrate (Millipore).

1.2. Proteins overexpression and purification.

Full length wild type NPM1, mutant A (NPM1MutA), and nucleophosmin spanning residues 1-188 (NPM1ΔC106), all with an N-terminal His-ZZ tag, were overexpressed in *E. coli* BL21 (DE3), and purified as in Arregi et al. (2015). Purification involved Ni-NTA chromatography, tags removal with TEV protease, reverse Ni-NTA and a final size exclusion chromatography (SEC) step. Histagged NPM1 core domain was a clone obtained from Dr. Se Won Suh (Lee et al., 2007). For purification of this construct, cells were disrupted by sonication in 25 mM Tris-HCl pH 7.5, 100 mM NaCl, 10% glycerol, 1mM DTT, supplemented with lysozyme (20 mg/L culture) and a cocktail of protease inhibitors (Complete, EDTA-free, Roche). The clarified extract was loaded on a Ni-NTA affinity column (His Trap FF, GE Healthcare) and the protein eluted with an imidazole gradient. Then it was further purified by gel filtration chromatography with Superdex 200 (GE Healthcare) in 25 mM Tris-HCl pH 7.5, 100 mM NaCl, concentrated and frozen for storage. APE1 (full length and APE1ΔN33) was subcloned in the same plasmid as NPM1 (pTGA20) and purified using the same chromatographic steps. SEC was done in buffer 25 mM Tris-HCl pH 7.5, 100 mM NaCl, 1 mM DTT, 10% glycerol. After purification, all proteins were concentrated, flash frozen with liquid nitrogen and stored at -80 ºC. They were quantified with NanoDrop 2000 (Thermo Scientific), based on ε_{280} as calculated with ProtParam (Gasteiger et al., 2005).

1.3. DNA oligonucleotides.

As model of abasic DNA, we used a dumbbell-shaped oligonucleotide of 46 residues, with a centrally located tetrahydrofurane (THF) (Freudenthal et al., 2015) 5´-CTGGAGCTTGCTCCAG CGCXCGGTCGATCGTA AGATCGACCGTGCG-3′, where X represents THF), synthesized by IDT (Leuven, Belgium). For anisotropy

binding assays, a fluorescein-labelled (in thymine 28) oligo with the same sequence was used. To prepare the "substrate" ("Dumbbell S" or "Dumbbell SF" when fluorescently labelled), the oligos were resuspended at 100 μM in water, annealed by heating 5 min at 95 ºC and slowly cooling down in a thermoblock, and ligated with T4 ligase (New England Biolabs) (4000 U ligase per nmol of DNA). Ligation of near 100% of the DNA was confirmed by denaturing polyacrylamide-urea electrophoresis (see section 2.8). For activity and binding assays the DNA was purified from ligase and magnesium with the "Nucleotide Removal Kit" (QIAGEN) and re-annealed; this could not be done for CD and FT-IR, though, since due to the higher amount needed, the lost of yield was too high to be afforded. FT-IR spectra, most CD measurements and also some binding assays were performed with a model of product DNA ("Dumbbell P" and "Dumbbell PF", respectively) (Freudenthal et al., 2015), with the same sequence as the substrate but starting with 5´ THF.

1.4. Native electrophoresis.

Samples containing a fixed concentration of NPM1 and increasing amounts of APE1 in buffer 20 mM potassium phosphate, 50 mM NaCl, 5 mM $MgCl_2$, 2 mM DTT, 0.01% (w/v) Tween-20, pH 7.0 (total volume of 20 μL) were incubated for 30 min at room temperature and loaded in precast native 4-16% polyacrylamide (PA), 10 wells Bis-Tris gels (Invitrogen). Running buffer and sample buffer (without G-250) were also from Invitrogen. Gels were run for 130 min at 150 V at 4 ºC, stained with Coomassie solution, and photographed with Gel Doc EZ System (Bio-Rad). Densitometry analysis of the protein bands was performed with Quantity One (Bio-Rad), and the measured intensities were fitted to a quadratic function to obtain a binding curve. 3-5 experiments were averaged to estimate K_D values. Ternary mixtures NPM1/APE1/DNA were also analyzed by native electrophoresis using the same conditions, but in this case gels were also stained with GelRed (Biotium) prior to Coomassie.

1.5. Isothermal titration calorimetry (ITC).

NPM1/APE1 binding was measured with a Nano-ITC (TA instruments) (Low Volume, with a cell of 189 μL). Both proteins were dyalized in buffer 20 mM potassium phosphate, 50 mM NaCl, 5 mM $MgCl_2$, 2 mM TCEP, pH 7.0, centrifuged and degassed prior to the measurement. 200-500 μM APE1, was titrated onto NPM1, either wild type

or mutant A (5-30 μM pentamer), in 33 injections of 1.5 μL, at 20 ºC. Dilution controls were performed diluting APE1 into buffer. For baseline correction, the average of the heat of the 3 last injections was substracted from the isotherm. Isotherms were analyzed with the Nano Analyze software (TA), using a model of independent binding sites.

1.6. Circular dichroism (CD).

Circular dichroism measurements were performed in a Jasco 720 spectropolarimeter equipped with Peltier temperature control, in a cuvette of 0.2 cm pathlength, in buffer 20 mM potassium phosphate pH 7.0, 50 mM NaCl, and either 0.5 mM EDTA or 5 mM $MgCl_2$. Concentrations were 4 ㎜ of NPM1, APE1 or oligo. Temperature scans were done at 60 ºC /h.

1.7. Fourier transform infrared (FT-IR) spectroscopy.

For infrared spectroscopy, samples contained 100 μM (or 50 μM, in the mixtures with DNA) APE1, either alone, or in the presence of equimolar amounts of NPM1 pentamer or DNA oligo ("product"). The corresponding control samples of NPM1 and DNA were also measured. For H/D exchange, samples were subjected to 6-7 cycles of concentration with Amicon Ultra 0.5 mL filter units (Millipore) of 10 K cuttoff (except for DNA alone, where 3K was used), and dilution in D_2O buffer (20 mM potassium phosphate, 50 mM NaCl, 5 mM $MgCl_2$, 2 mM DTT, 0.01% (p/v) Tween-20, pD 7.0). The final concentration was checked by UV absorption and readjusted as necessary. Spectra were recorded in a Thermo Nicolet 5700 spectrometer equipped with a MCT detector using a Peltier-based temperature controller with 25 μm-pathlength calcium fluoride cells (BioTools). A 25-μl sample aliquot was deposited on a cell that was sealed with a second cell. Typically 370 scans were collected for each background and sample, and the spectra were obtained with a nominal resolution of 2 cm^{-1}. Temperature was increased at a rate of 1 °C min^{-1} between 20 and 80 °C for all samples.

1.8. APE1 incision assays.

Incision of 5 μM abasic DNA model oligonucleotide (Dumbbell S) was assayed in buffer 20 mM potassium phosphate, 50 mM NaCl, 5 mM $MgCl_2$, 2 mM DTT, pH 7.0, in the presence or absence of 5 μM NPM1, and monitorized by denaturing 18% polyacrylamide (PA)-urea gels (Adachi et al., 2015). The assay was done either as a function of APE1 concentration (0-200 pM) in reactions of 15 min at 37 ºC, or as a

function of time ("steady state kinetics"), incubating samples during 0-30 min at 37 ºC in the presence of 5 nM APE1. In all cases, the reaction was halted by addition of the same volume of loading solution containing 96% formamide, 10 mM EDTA and 0.1% bromophenol blue, and heating the sample at 95ºC for 5 min, prior to electrophoresis. 10 well, 1 mm thick, 18% PA gels containing 8 M urea were prerun for 30 min, loaded with 20 μL of sample per well, and run during 140 min at 175 V. Gels were stained with GelRed and densitometrically analyzed with Gel Doc EZ and Quantity One (Bio-Rad).

1.9. APE1-DNA binding assays based on fluorescence anisotropy.

To analyze DNA binding, 10 nM fluorescein-labelled oligo (Dumbbell SF) was mixed with 0-10 μM APE1 in buffer 20 mM potassium phosphate, 50 mM NaCl, 2 mM DTT, pH 7.0, containing 10 mM EDTA, incubated for 15 min at room temperature, and the anisotropy at 520 nm was measured in an SLM 8100 fluorimeter (Aminco). In some experiments, 5 μM NPM1 was added prior to the incubation. Binding curves were fitted to a quadratic function to estimate K_D.

2. Results

2.1. Upon oxidative damage, NPM1 partly translocates to insoluble chromatin patches, resembling APE1 behaviour.

APE1 has been described to exit the nucleoli and settle on repair patches, which are resistant to extraction of soluble proteins with a detergent-containing buffer ("CSK buffer"), upon treatment of HeLa cells with the oxidative agent $KBrO_3$ (Campalans et al., 2013). We have corroborated this observation using either APE1-EGFP or APE1-mCherry (Fig. S1): whereas in untreated HeLa cells, all of the APE1 is washed away by the buffer containing 0.5% Triton X-100, after treatment with $KBrO_3$ (300 mM during 30 min), APE1 remains unsolubilized and distributed through nucleoplasm and partly cytoplasm. To see whether NPM1 localization is also sensitive to oxidative conditions, we have analyzed the localization of YFP-NPM1 in HeLa cells coexpressing APE1-mCherry treated with $KBrO_3$ and solubilized with CSK buffer prior to fixation. In basal conditions, we found that NPM1 is almost entirely nucleolar, as expected, and that it remains resistant to the solubilizing treatment, reflecting a firm attachment to nucleolus. By contrast, exposure to $KBrO_3$ induces spreading of NPM1 through nucleoplasm (Fig. 1). NPM1 exit from nucleolus nicely correlates with the behaviour of APE1; moreover,

the staining pattern of both proteins is (not uniform through nucleoplasm), and reflects that they accumulate in the same nuclear regions. These areas probably correspond to open euchromatin, based on DAPI staining. It has been described that "BER repair takes place in low density chromatin regions (Campalans et al., 2013). The similar behaviour, localization and resistance to detergent solubilization of both NPM1 and APE1 suggest-that NPM1 might be recruited to the same structures ("*patches*", or "*BERosomes*" or repair complexes) as described for APE1 (Campalans et al., 2013), and furthermore, that both proteins might interact in the context of BER repair.

We have observed that oxidative damage with H_2O_2 does not elicit the same effects neither in APE1 nor NPM1 (Fig. S2), suggesting that the co-localization of both proteins in patches (and potentially, their interaction there) might be specific of damage associated with the generation of 8-oxoguanine, such as that caused by $KBrO_3$ treatment (Ballmaier et al., 2006).

2.2. Nucleolar exit of NPM1 upon oxidative stress may be mediated by Thr199 phosphorylation.

It is well established that endogenous NPM1 is mainly nucleolar, with particular enrichment in the periphery of nucleoli (Fig. 2A). By contrast to the localization of the general pool of NPM1, detection of NPM1 phosphorylated at T199 (NPM1p199) *via* a specific antibody results in a remarkably different staining: NPM1p199 is completely excluded from nucleoli (Fig. 2A), as it had been previously shown by Koike et al. (2010). Interestingly, we have observed that a phosphomimicking mutant where T199 has been substituted for Asp, NPM1T199D, cannot reproduce the behaviour of NPM1p199, i.e., its localization is identical to overexpressed wild type NPM1 (Fig. S3), suggesting that in this case, the mechanistic effect of the phosphorylation does not merely depend on the presence of a negative charge.

NPM1p199 has been found within the DSBs repair *foci* on chromatin (Koike et al., 2010). Therefore, an increase in the phosphorylated form upon induction of such lesions of DNA could be expected. By immunoblotting of extracts from cells either untreated or subjected to different genotoxic insults, we have observed, however, that the chemotoxic agent neocarzinostatin (NCS), which induces DSBs and accumulation of repair *foci* in the chromatin (Olazabal-Herrero et al., 2016) does not enhance the amount of NPM1p199 (Fig. 2B). By contrast, treatment of the cells with $KBrO_3$ greatly

increases the amount of phosphorylated protein (Fig. 2B). Interestingly, this increase in NPM1p199, dependent on $KBrO_3$ concentration, does not affect the total content of NPM1, thus reflecting a net change in phosphorylation status (Fig. 2C). For comparison, we have also treated the cells with the microtubule disruptor nocodazole. This drug causes synchronization of the cell cycle in mitosis (Ma & Poon, 2017), when the concentration of NPM1p199 peaks (Zou et al., 2008). Treatment of cells with either $KBrO_3$ or nocodazole similarly increases the quantity of NPM1p199 (Fig. 2B-D). These results indicate that oxidative stress elicits phosphorylation of NPM1 at T199, and that this modification may signal or favour NPM1 release from nucleoli.

2.3. NPM1 and APE1 form complexes *in vitro*.

The correlation between NPM1 and APE1 behaviours in the context of oxidative damage with $KBrO_3$ suggested that both proteins might co-operate in BER repair, and prompted us to characterize their interplay in detail. An interaction between NPM1 and APE1 has been described (Vascotto et al., 2009). To explore this interaction, we have analyzed the formation of complexes between the recombinant proteins. An SDS-PAGE of all the constructs we have studied is shown in Fig. S4, and schematic drawings thereof in Fig. S5.

NPM1 displays characteristic multiple bands in native PAGE (Fig. 3). We have checked that our purified nucleophosmin behaves as a homogeneous species in denaturing PAGE (Fig. S4) and analytical ultracentrifugation (unpublished results). Furthermore, migration in multiple bands has been previously described for native NPM1 extracted from human cells (Chan & Chan, 1995). Therefore, we attribute the migration pattern to conformational variability of NPM1 pentamer mediated by the flexible linkers. On the other hand, whereas at the pH of the assay (7.5), positively charged APE1 does not enter the gel, in mixtures of NPM1 with increasing concentrations of APE1, a new species that migrates slower than free NPM1 is accumulated (Fig. 3A, B). This band probably corresponds to a stable complex of NPM1 and APE1, of larger size, and less charge than NPM1 alone. Gel densitometry analysis shows saturation of the intensity of the band corresponding to the complex, indicating a specific interaction and allowing estimation of a K_D value of 0.4 ± 0.1 μM (Fig. 3C). Interestingly, the ladder of migration levels at intermediate saturation positions suggests that the stoichiometry of the complex could be of several (possibly 5) molecules of APE1 per NPM1 pentamer. When the experiment is done at 1 μM NPM1, i.e. a concentration above the estimated

K_D (Fig. 3D), the saturation is attained at a ca. 5-time excess of APE1, further pointing to a stoichiometry of 5 APE1 per NPM1.

We have also analyzed NPM1/APE1 binding by isothermal titration calorimetry (ITC). The binding of NPM1, negatively charged at neutral pH, to APE1, rich in basic residues, especially in the N-terminal segment, putatively involved in the recognition (Vascotto et. al., 2009; Fantini et al., 2010), may be expected to be driven by electrostatic forces, i.e. enthalpically driven. The titration of APE1 onto NPM1 (Fig. 4) is however, endothermic, meaning that the interaction is entropically driven. This observation suggests that there may be enthalpic cost (and entropic benefit) of desolvating charged groups, and/or hydrophobic contributions to the binding. It must be noted that NPM1 exhibits an inhomogeneous behaviour probably due to the interplay between differently charged regions of the molecule, which promote homotypic and heterotypic interactions (Mitrea et al., 2018). This property precludes, at the high NPM1 concentrations used in ITC measurements (approximately 20 μM pentamer), reliable determination of binding parameters, and could be the reason why the apparent affinity (K_D 13.3 ± 8.5 μM) (Table I) is lower than that estimated by native electrophoresis and densitometry. On the other hand, discrepancies between binding parameters yielded by ITC and other techniques (e.g. fluorescence) can be due to protein rearrangements subsequent to the initial interaction event. Such rearrangements or "induced fit", which result in a higher final affinity, may be too slow as to be detected in the ITC experiment but can instead be observed when a technique involving longer incubation times is used. The apparent stoichiometry obtained (2.3 ± 0.8 molecules of APE1 per NPM1 pentamer) is also unexpected. An alternative explanation for these binding parameters is that they are apparent values for binding to 5 identical binding sites with intervening negative cooperativity.

2.4. Contribution of the different protein domains and consequences of oncogenic mutations of NPM1 on the interaction with APE1.

To evaluate the role of different regions of NPM1 in the interaction with APE1, we have compared the binding of full length NPM1 with that of the isolated NPM1 core domain (the N-terminal, pentameric, 125 residues long region) (Fig. S5). NPM1 core displays a significantly lower ability to bind APE1 (K_D 8.8 ± 3.2 μM) (Fig. 5A). Although the interaction with APE1 had been described to rely on NPM1 core domain (Vascotto et al., 2009), our results indicate that this region is not enough for proper

binding of NPM1 to APE1.

To know which other regions of NPM1 are involved in APE1 recognition, we also evaluated the binding of a NPM1 truncated mutant (NPM1ΔC106), lacking the C-terminal globular domain and a preceding segment, both of them rich in Lys, Arg residues (Mitrea et al., 2018) (Fig. S5). We found that NPM1ΔC106 binds APE1 with an apparent K_D of 0.7 ± 0.2 μM, i.e. an affinity not significantly different from wild type NPM1 (Fig. 5A). Therefore, the C-terminal domain and the distal, positively charged part of the linker (residues 189-245) are dispensable for binding APE1.

In order to evaluate the consequences of AML-linked mutations of NPM1 on the interaction with APE1, we analyzed the binding properties of NPM1mutA (Arregi et al., 2015), the most common NPM1 variant in AML with mutated, cytoplasmic, NPM1 ("NPM1c+"). The mutations prevent the proper folding of the C-terminal domain and, since they conform to a nuclear export signal (NES), dictate the exacerbated export of the protein to the cytoplasm in AML cells (Federici and Falini, 2013; Arregi et al., 2015). Based on the electrophoretic binding assay, the mutant displays a slightly lower affinity for APE1 (K_D 0.9 ± 0.2 μM), as compared to wild type NPM1 (Fig. 5A). One must take into account that, due to its defective folding, our preparations of this mutant suffer from severe proteolytic degradation (Arregi et al., 2015) (Fig. S4); so any quantitative comparison must be taken with caution. We have also measured APE1 binding to NPM1MutA by ITC, obtaining similar apparent binding parameters as wild type NPM1 (Table I). Therefore, we conclude that AML-related mutations do not significantly affect APE1 binding ability of NPM1, and that an intact, folded C-terminal domain is not required for recognition of APE1. Statistical analysis of the binding of the four NPM1 constructs to APE1 indicates that wild type NPM1, NPM1MutA and NPM1ΔC106 all bind with the same affinity to APE1, while the isolated core domain is clearly not sufficient for binding. Altogether, our results indicate that, in addition to the NPM1 core domain (Vascotto et al., 2009), also the proximal region of the linker, but not the C-terminal 106 residues, are essential for APE1 recognition.

On the other hand, we have evaluated the NPM1 binding ability of a truncated mutant of APE1 lacking the first 33 N-terminal residues (APE1ΔN33). APE1 N-terminal region, rich in basic residues and not visible in APE1 crystal structures (i.e. conformationally mobile), has been previously found to be required for binding to

NPM1 (Vascotto et al., 2009). Our native electrophoresis-based binding assays indicate that, indeed, the absence of the positively charged N-terminal segment significantly reduces the affinity of APE1 for NPM1 (resulting in a K_D value of 14.4 μM, as compared with 0.4 μM for wild type APE1), but binding is not completely abrogated (Fig. 5B). Altogether, our results reveal that other regions of NPM1 and APE1, apart from the previously proposed ones, participate in the interaction.

2.5. APE1 conformation is sensitive to DNA binding.

We have analyzed the impact of binding to magnesium cofactor, abasic DNA, and/or NPM1 on APE1 conformational stability through circular dichroism (CD) and Fourier transform infrared (FT-IR) spectroscopies. Human full length APE1, in the absence of magnesium, displays a far-UV circular dichroism spectrum (not shown) compatible with its α/β structure (Mol et al., 2000), and a thermal denaturation T_m of 48 ºC (Fig. 6). Addition of 5 mM $MgCl_2$ renders APE1 more stable, increasing its denaturing temperature to 52 ºC (Fig. 6). This thermal stabilization, in agreement with previously reported data based on differential scanning fluorimetry (He et al., 2014) suggests that binding to the metal ion, in spite of not inducing gross changes in the crystal structure of APE1 (He et al., 2014), promotes its compactness.

To analyze the effect of abasic DNA binding on APE1 conformation, we have used an oligonucleotide containing an abasic analog (tetrahydrofurane, THF) in the 5´terminus, mimicking APE1 "product" (Freudenthal et al., 2015) (Fig. S5~~3~~). Binding to this DNA ("Dumbbell P") induces a significant thermal stabilization of APE1, which is patent both in the absence (0.5 mM EDTA) as in the presence of magnesium (5 mM), the unfolding T_m shifting from 48 to 60 ºC, and from 52 to 61.5 ºC, respectively (Fig. 6). APE1 crystal structures (most of them obtained at acidic pH) have shown that the protein does not suffer relevant changes when it binds to abasic DNA, either substrate or product (Mol et al., 2000; Freudenthal et al., 2015). On the contrary, APE1 has been described to maintain a rigid, pre-formed binding surface optimally suited to recognize the abasic site (Mol et al. 2000). Nevertheless, the significant thermal stabilization we observe (in solution, at a pH compatible with activity) argues that the protein conformation or dynamics somehow senses the binding. To explore in deeper detail the consequences of complex formation with the DNA, we have used FT-IR. Interestingly, APE1 Amide I band (between 1700 and 1600 cm-1), sensitive to protein secondary structure, reveals changes upon binding to the DNA (Fig. 6B). These minor changes,

accounting for 10-15% of the peptide bonds, might be thought to correspond to rearrangements of the N-terminal flexible region, not visible in the crystal structures. We have also analyzed the CD and FT-IR spectra as well as thermal stability with and without DNA of the truncated form of APE1, lacking the N-terminal 33 residues (APE1ΔN33), which is catalytically active (Mol et al., 2000; Lirussi et al., 2012). Binding of APE1ΔN33 to the oligo Dumbbell P also results in similar alterations of the Amide I band (Fig. 6B) and thermal stability, as followed either by ellipticity at 222 nm (not shown) or width of the Amide I band (Fig. S64). Therefore, the changes induced by DNA binding cannot be assigned to the N-terminal 33 residues, but perhaps to the following ca. 30 residues region, also flexible, and/or protein loops. Overall, and in line with previous reports (Yu et al., 2010) our data indicate that APE1 (either full length or isolated globular domain) conformation or dynamics is sensitive to abasic DNA binding.

We have also explored the conformational consequences of APE1/NPM1 complex formation, using wild type APE1 and the truncated mutant NPM1ΔC106, which as mentioned, is sufficient for binding, but lacks thermal transitions in the 20-80ºC range. At concentrations well above the K_D, we could not observe any change neither in the spectral properties of both proteins, nor in the thermal profile of APE1 (not shown). This observation supports the notion that NPM1 binds mainly to the N-terminal segment of APE1, as described (Vascotto et al., 2009), having little effect on the conformation of APE1 globular, major domain. Finally, in ternary mixtures APE1/DNA/ NPM1ΔC106 we could not observe any effect of NPM1 on the DNA-bound APE1 conformation or on the stabilization brought about by DNA (not shown).

2.6. NPM1 favours the specific binding of APE1 to abasic substrate DNA.

To get insight into the putative regulatory role of NPM1 on APE1 catalysis, we have analyzed the effect of NPM1 on the recognition and catalytic incision of an abasic DNA by APE1. First we have confirmed that our preparation of recombinant APE1 is highly active cleaving the model oligonucleotide of abasic DNA (Dumbbell S), as followed by denaturing polyacrylamide-urea DNA electrophosresis (Fig. 7A). In line with the reported stimulation of APE1 incision by NPM1 (Vascotto et al., 2009), but observing a greater effect than in their report, we have found a higher endonuclease activity in the presence of NPM1 (Fig. 7A).

In order to investigate the molecular basis of this activation, we have explored the effect of NPM1 on APE1 binding to the abasic DNA substrate. It had been previously described (Maher & Bloom, 2007; Freudenthal et al., 2015) that APE1 binds with high affinity abasic DNA and also binds, albeit with lower affinity, the product, nicked DNA, which has been related to a physiologically advantageous slow release of cytotoxic incised BER intermediates during DNA damage processing (Maher & Bloom, 2007). We have measured the binding by monitoring the increase in fluorescence anisotropy of fluorescein-labelled DNA upon addition of increasing amounts of APE1. The affinity we have determined for APE1 binding to the oligo Dumbbell S (K_D 39 ± 8 nM (Fig. 7B,C) is similar to previously reported data with abasic-mimicking oligonucleotides (Hadi et al., 2000), but lower than that determined by Freudenthal et al. (2015) with the same DNA sequence that we have used. This could be explained because they use a buffer of lower ionic strength and/or we could not get reliable readings at a DNA concentration sufficiently below the K_D. When the titration is performed in the presence of an excess of NPM1, no additional increase in the anisotropy is obtained, suggesting that NPM1 regulatory effect is not mediated by formation of a ternary complex DNA / APE1 / NPM1 (Fig. 7B). On the contrary, at high APE1 concentration, the maximum anisotropy value attained is lower in the presence of NPM1, suggesting that NPM1 can compete with the low-affinity, off-target binding of APE1 to DNA. However, APE1 affinity for the specific site on DNA (supposedly the abasic site-mimicking THF) is slightly enhanced in the presence of NPM1 (Fig. 7C), rendering a K_D value of 25.3 ± 8 nM, as compared to 39 ± 8 nM in the absence of NPM1 (p value < 0.05).

We have also explored the formation of complexes in ternary mixtures of APE1, DNA and NPM1 through native gel electrophoresis (Fig. 8). With equimolar concentrations of APE1 and the "product" abasic DNA (Dumbbell P), a defined band, probably corresponding to a 1:1 complex can be detected (Fig. 8A), while at higher APE1:DNA ratios (4:1) an heterogeneous species, putatively containing more molecules of APE1 bound to off-target sites is obtained (Fig. 8B). The addition of NPM1 partly competes with the heterogeneous, off-target binding, but not with the specific complex (Fig. 8A,B). On the contrary, when the different bands are analyzed by densitometry, it can be concluded that NPM1 favours the formation of the APE1:DNA (1:1) complex, either if its quantity is followed based on Coomassie staining (protein amount) or GelRed (DNA). Collectivelly, these results suggest that NPM1 may be able to favour the formation of a specific, discrete APE1:abasic DNA complex, opposing to alternative,

off-target APE1:DNA interactions. Apparently, this selection for the specific, productive binding results in a higher affinity for abasic DNA (Fig. 7C) and, ultimately, in the stimulation of APE1 activity (Fig. 7A).

3. Discussion

Our results indicate that, under certain oxidative stress conditions, i.e. $KBrO_3$ treatment, NPM1 is partly released from nucleoli and remains in chromatin regions (probably euchromatin), which might correspond to DNA damage repair platforms. Nucleoplasmic translocation of NPM1 upon a number of different stresses, including oxidative damage, has been previously reported (Colombo et al., 2011; Yang et al., 2016; Sekhar et al., 2014) and seems a common theme in the response to cellular perturbations of this and other nucleolar proteins (Antoniali et al., 2014; Scott & Oeffinger 2016). Moreover, NPM1 localization dynamics has been proposed to depend on posttranslational modifications (the protein is amenable to regulation by phosphorylation, ubiquitylation, sumoylation, acetylation, PARylation, etc). In this sense, we have observed that the oxidative treatment induces phosphorylation of NPM1 at least on T199. This modification perhaps reduces the affinity of the protein for G-quadruplex forming DNA sequences in the nucleolus, prompting nucleolar release upon DNA damage. Thus, phosphorylation of NPM1 would be related not only with DSBs repair (Koike et al., 2010), but also with repair of oxidative damage. Recently, glutathionylation of a Cys residue in the C-terminal domain of NPM1 has been described as a mechanism underlying nucleolar oxidation state sensing and release from nucleolus (Yang et al., 2016). The multiple posttranslational modifications affecting NPM1 might impact in different ways its localization dynamics and DDR-related activities.

The exact role of NPM1 in BER is so far unknown. The participation of NPM1 in this and several other DDR pathways might be related to the histone chaperoning activity of the protein, since chromatin remodelling must be a requirement in all repair processes. On the other hand, the nucleolar enrichment in normal conditions of both NPM1 and APE1, and the fact that they are able to bind not only DNA but also RNA, and indeed display enzymatic activities on RNA, at least *in vitro*, has inspired the notion that they might collaborate in RNA quality control activities in addition to DDR (Antoniali et al., 2014). Moreover, our data point to a direct role of NPM1 in the BER machinery. The

similarity between the behaviour of NPM1 and APE1 when the cells are subjected to oxidation (dependence on $KBrO_3$ concentration, localization within certain nuclear regions, and resistance to detergent- solubilization) strongly suggests that NPM1 could be recruited to the same structures on chromatin as APE1 (Campalans et al., 2013), i.e., platforms where active BER is taking place.

If NPM1 is involved in BER regulation, the interaction between NPM1 and APE1 may be relevant as pharmacological target (Poletto et al., 2015), since interfering with DNA repair represents a cancer therapy strategy. An *in vitro* interaction between NPM1 and APE1 has been described implying the N-terminal, core domain of NPM1, and the flexible, N-terminal region of APE1 (Vascotto et al., 2009; Poletto et al., 2013). In our further characterization of the NPM1/APE1 association, we demonstrate a specific binding where part of the linker region of NPM1 (but not the region comprising the 106 last residues, including the C-terminal domain) is involved, explaining the ability of the AML leukaemia-related NPM1 mutant to also bind APE1 and apparently sequester it when aberrantly locating in the cytoplasm of AML cells (Vascotto et al., 2014, and our unpublished observations). In addition, we have found that more than one molecules of APE1 can bind to one NPM1 pentamer, and that the interaction is entropically driven. Although unfortunately we could not obtain evidences of an interaction between the two overexpressed proteins in cells, using the new "F2H" technology (from ChromoTek) (unpublished results), an *in vivo* association has been reported based on proximity ligation assay (PLA) (Poletto et al., 2013). It remains to be seen whether phosphorylation of NPM1 at Thr199, which according to our data correlates with nucleolar release, or further posttranslational modifications of either NPM1 or APE1 could modulate / enhance the association.

NPM1 stimulates APE1 cleavage of abasic DNA (Fig. 7A, Vascotto et al., 2009), while interestingly, it has been described to inhibit APE1 endonuclease activity on RNA (Vascotto et al., 2009). The *in vitro* NPM1 regulatory effects, along with the similarity between the localization dynamics behaviour of both proteins (Fig. 1) suggest that NPM1 might participate in repair tasks on BER patches. Tell and co-workers have proposed that acetylation of Lys residues in APE1 would inhibit the association to NPM1 under stress conditions. Nevertheless, the same authors have reported "proximity ligation assay" (PLA) signal also outside the nucleoli; thus we think that an interaction between both proteins (even if the binding mode might differ) within the BER

machinery is feasible and could imply a modulation of APE1 functionality. The molecular basis of such regulation remains nevertheless elusive.

We have found that NPM1 can compete with low-affinity, off-target APE1 binding to DNA, and could select for the specific, productive APE1/DNA complex. NPM1 interacts with the N-terminal flexible region of APE1 (Vascotto et al., 2009, and this study). This segment, ca. 40 residues long, has been related to regulation of DNA and /or RNA binding (Fantini et al., 2010; Poletto et al., 2013), and could be necessary for APE1 scanning of DNA to search target lesions, as disordered tails of other DNA-binding proteins (Vuzman et al., 2000). NPM1, by binding to APE1 N-terminal segment, could maintain APE1 in an open conformation, ready for productive association to abasic sites. This might be perhaps promoted under cellular conditions of heavy damage. NPM1 has been also proposed to regulate NF-κB activity on DNA by keeping this protein in an open conformation (Lin et al., 2017). The modulation exerted by NPM1 resembles the role of other chaperones, in the sense that their activity is only evident *in vitro* at high chaperone: target protein ratios (Sharma et al., 2010), as it is the case in our experiments, where there is a significant molar excess of NPM1.

We have shown that, upon binding to an abasic product-mimicking DNA, APE1 suffers conformational changes and becomes significantly stabilized, thus probably more compact. In line with this notion, it had been described, based on mass spectrometric protein footprinting, that binding to DNA after incision results in protection of some APE1 Lys residues (Yu et al., 2010). According to that study, APE1 conformation is still more "tensioned" when bound to the substrate, and then partly "relaxes" once the incision of the DNA has taken place, perhaps in order to facilitate discharge from DNA. Although in our experiments we could not demonstrate NPM1 competition with APE1 binding to the abasic product, NPM1, by grasping the N-terminal region of APE1 and acting on it as a lever, might somehow favour the release of APE1 from DNA once incised. This might be facilitated, *in vivo*, by subsequently intervening enzymes of the BER pathway, so that the cleaved intermediate is not released until it can be properly handled (Almeida and-Sobol, 2007; Parsons and-Dianov, 2013; Freudenthal et al., 2015). Then APE1 would be ready to dismount from DNA and scan chromatin for another abasic site. Other proteins participating in the BER route (XRCC1, Polβ) have also been proposed to stimulate APE1 activity by releasing it from product inhibition (Vidal et al., 2001; Masuda et al., 1998).

4. Conclusions

Nucleophosmin (NPM1) interacts with the repair enzyme APE1 and is able to stimulate *in vitro* APE1 incision of abasic DNA, suggesting that it could take part in the BER pathway. Our finding that, upon oxidative damage to cells, part of nucleophosmin is released from nucleoli (being correlated with phosphorylation at Thr199) and recruited to insoluble patches on chromatin, resembling APE1 behavior, further supports this hypothesis. In this study, we have further characterized the interaction between NPM1 and APE1, showing that pentameric NPM1 can bind several molecules of APE1 with submicromolar affinity. Not only NPM1 core domain and APE1 N-terminal region, as previously proposed, but also the proximal part of NPM1 linker region and the globular domain of APE1 are required for proper binding. The fact that the NPM1 C-terminal 106 residues are dispensable for the recognition explains why the AML leukemia-associated NPM1 mutant keeps the ability to bind APE1, which might lead to APE1 mislocalization and pathogenic deregulation. We have also found that NPM1 is able to compete with APE1 off-target binding to DNA while favouring the specific, productive binding to the abasic site. This stimulatory effect, as well as a putative induction of APE1 release from the incised DNA, would positively regulate APE1 repair activity. In summary, our results depict a new, operational role of NPM1 in the modulation of BER machinery.

Funding

This work was funded by the Spanish Ministry of Economy and FEDER (grant SAF2014-57743-R), the Basque Government (grant IT709-13) and the University of the Basque Country (grant GIU18/172)

Author's contribution

SB designed the research. All of the authors performed the experiments. DJL, AdB, IdlA, JM and SB analyzed and interpreted the data. S.B. wrote the paper with the contribution of DJL and MAU.

Conflict of interest

The authors declare that they have no competing interests.

Acknowledgements

The authors thank the staff from the High Resolution Microscopy Facility (SGIker-UPV/EHU) for technical support, Dr. José Martínez (University of Granada) for advice on interpretation of ITC data, and Dr. José .Antonio. Rodríguez (University of the Basque Country) for suggestions and advice. A.dB. and M.G. were recipients of an Ikasiker fellowship (Basque Government).

References

Adachi H, Yu YT (2014) Purification of radiolabeled RNA products using denaturing gel electrophoresis. Curr Protoc Mol Biol 105, doi: 10.1002/0471142727.mb0420s105.

Almeida KH, Sobol RW. (2007) A unified view of base excision repair: Lesion-dependent protein complexes regulated by post-translational modification. DNA Repair 6, 695-711**,** doi:10.1016/j.dnarep.2007.01.009

Antoniali G, Lirussi L, Poletto M, Tell G. (2014) Emerging roles of the nucleolus in regulating the DNA damage response: the noncanonical DNA repair enzyme APE1/Ref-1 as a paradigmatical example. Antioxid Redox Signal. 2014 20(4):621-639, doi: 10.1089/ars.2013.5491

Arregi I, Falces J, Olazabal-Herrero A, Alonso-Mariño M, Taneva SG, Rodríguez JA, Urbaneja MA, Bañuelos S. (2015) Leukemia-Associated Mutations in Nucleophosmin Alter Recognition by CRM1: Molecular Basis of Aberrant Transport. PLoS One.: 10(6), doi: 10.1371/journal.pone.0130610.

Ballmaier D and Epe B (2006) DNA damage by bromate: mechanism and consequences. Toxicology 221, 166-171, doi: 10.1016/j.tox.2006.01.009.

Bañuelos S, Lectez B, Taneva SG, Ormaza G, Alonso-Mariño M, Calle X, Urbaneja MA. (2013) Recognition of intermolecular G-quadruplexes by full length nucleophosmin. Effect of a leukaemia-associated mutation. FEBS Lett. 587, 2254-2259, doi: 10.1016/j.febslet.2013.05.055.

Boisvert FM, van Koningsbruggen S, Navascués J, Lamond AI (2007) The multifunctional nucleolus. Nat Rev Mol Cell Biol 8(7), 574-585, doi: 10.1083/jcb.200702147.

Box JK, Paquet N, Adams MN, Boucher D, Bolderson E, O'Byrne KJ, Richard DJ. (2016) Nucleophosmin: from structure and function to disease development. BMC Mol Biol 17(1):19, doi: 10.1186/s12867-016-0073-9.

Campalans A, Kortulewski T, Amouroux R, Menoni H, Vermeulen W, Radicella JP. (2013) Distinct spatiotemporal patterns and PARP dependence of XRCC1 recruitment to single-strand break and base excision repair. Nucleic Acids Res 41, 3115–3129, doi:

10.1093/nar/gkt025.

Chan PK, Chan FY. (1995) Nucleophosmin/B23 (NPM) oligomer is a major and stable entity in HeLacells. Biochim Biophys Acta 1262, 37-42.

Chiarella S, De Cola A, Scaglione GL, Carletti E, Graziano V, Barcaroli D, Lo Sterzo C, Di Matteo A, Di Ilio C, Falini B, Arcovito A, De Laurenzi V, Federici L. (2013) Nucleophosmin mutations alter its nucleolar localization by impairing G-quadruplex binding at ribosomal DNA. Nucleic Acids Res. 41(5):3228-3239, doi: 10.1093/nar/gkt001.

Colombo E, Marine JC, Danovi D, Falini B, Pelicci PG (2002) Nucleophosmin regulates the stability and transcriptional activity of p53. Nat Cell Biol 4, 529–533, doi: 10.1038/ncb814.

Colombo E, Bonetti, P, Denchi EL, Martinelli P, Zamponi R et al. (2005) Nucleophosmin is required for DNA integrity and p19Arf protein stability. Mol Cell Biol 25, 8874–8886, doi: 10.1128/MCB.25.20.8874-8886.2005.

Colombo, E., Alcalay, M. & Pelicci, P. G. (2011) Nucleophosmin and its complex network: a possible therapeutic target in hematological diseases. Oncogene 30, 2595-2609, doi: 10.1038/onc.2010.646.

Emmott E and Hiscox JA (2009) Nucleolar targeting: the hub of the matter. EMBO Rep 10(3), 231-238, doi: 10.1038/embor.2009.

Falini B, Mecucci C, Tiacci E, Alcalay M, Rosati R et al. (2005) Cytoplasmic nucleophosmin in acute myelogenous leukemia with a normal karyotype. N Engl J Med 352: 254-266, doi: 10.1056/NEJMoa041974.

Fantini D, Vascotto C, Marasco D, D'Ambrosio C, Romanello M, Vitagliano L, Pedone C, Poletto M, Cesaratto L, Quadrifoglio F, Scaloni A, Radicella JP, Tell G. (2010) Critical lysine residues within the overlooked N-terminal domain of human APE1 regulate its biological functions. Nucleic Acids Res. 38(22):8239-56, doi: 10.1007/s00018-010-0486-4.

Federici L, Falini B (2013) Nucleophosmin mutations in acute myeloid leukemia: a tale of protein misfolding and mislocalization. Protein Sci 22: 545-556, doi:

10.1002/pro.2240.

Freudenthal BD, Beard WA, Cuneo MJ, Dyrkheeva NS, Wilson SH. (2015) Capturing snapshots of APE1 processing DNA damage. Nat Struct Mol Biol 22: 924-931, doi: 10.1038/nsmb.3105.

Gasteiger E, Hoogland C, Gattiker A, Duvaud S, Wilkins M.R, Appel R.D, Bairoch A. (2005) Protein Identification and Analysis Tools on the ExPASy Server. In: John M. Walker (ed): The Proteomics Protocols Handbook, Humana Press, 571-607.

Grisendi S, Mecucci C, Falini B, Pandolfi PP. (2006) Nucleophosmin and cancer. Nat. Rev. Cancer 6, 493-505, doi: 10.1038/nrc1885.

Grummitt CG, Townsley FM, Johnson CM, Warren AJ, Bycroft M (2008) Structural consequences of nucleophosmin mutations in acute myeloid leukemia. J. Biol. Chem. 283, 23326-23332, doi: 10.1074/jbc.M801706200.

Guillonneau M, Paris F, Dutoit S, Estephan H, Bénéteau E, Huot J, Corre I (2016) Oxidative stress disassembles the p38/NPM/PP2A complex, which leads to modulation of nucleophosmin-mediated signaling to DNA damage response. FASEB J. 30(8):2899-2914, doi: 10.1096/fj.201500194R.

Hadi MZ, Coleman MA, Fidelis K, Mohrenweiser HW and Wilson 3rd DM (2000) Functional characterization of Ape1 variants identified in the human population. Nucleic Acids Res. 28, 3871-3879, doi: 10.1093/nar/28.20.3871.

He H, Chen Q, Georgiadis MM. (2014) High-resolution crystal structures reveal plasticity in the metal binding site of apurinic/apurymidinic endonuclease I Biochemistry 53(41), 6520-6529, doi: 10.1021/bi500676p.

Jackson EB, Theriot CA, Chattopadhyay R, Mitra S, Izumi T. (2005) Analysis of nuclear transport signals in the human apurinic/apyrimidinic endonuclease (APE1/Ref1) Nucleic Acids Res. 33(10), 3303-3312, doi: 10.1093/nar/gki641.

Kennedy MJ, Hughes RM, Peteya LA, Schwartz JW, Ehlers MD, Tucker CL. (2010) Rapid blue-light-mediated induction of protein interactions in living cells. Nat Methods 7(12), 973-975, doi: 10.1038/nmeth.1524.

Koike A, Nishikawa H, Wu W, Okada Y, Venkitaraman AR et al. (2010) Recruitment of

phosphorylated NPM1 to sites of DNA damage through RNF8-dependent ubiquitin conjugates. Cancer Res 70, 6746-6756, doi: 10.1158/0008-5472.CAN-10-0382.

Krokan H.E. and Bjørås, M. (2013) Base excision repair. Cold Spring Harb Perspect Biol 5:a012583, doi: 10.1101/cshperspect.a012583.

Lee HH, Kim HS, Kang JY, Lee BI, Ha JY, Yoon HJ, Lim SO, Jung G, Suh SW. (2007) Crystal structure of human nucleophosmin-core reveals plasticity at the pentamer-pentamer interface. Proteins 69:672-678, doi: 10.1002/prot.21504.

Lee SY, Park JH, Kim S, Park EJ, Yun Y, Kwon J. (2005) A proteomics approach for the identification of nucleophosmin and heterogeneous nuclear ribonucleoprotein C1/C2 as chromatin-binding proteins in response to DNA double-strand breaks. Biochem J.388(Pt 1), 7-15, doi: 10.1042/BJ20042033.

Li M. and Wilson D.M. (2014) Human apurinic/apyrimidinic endonuclease 1. Antioxidants Redox Signal. 20: 678-699, doi: 10.1089/ars.2013.5492.

Lin J, Kato M, Nagata K, Okuwaki M (2017) Efficient DNA binding of NF-kB requires the chaperone-like function of NPM1. Nucleic Acids Res. 45, 3707-3723, doi: 10.1093/nar/gkw1285

Lindström M.S. (2011) NPM1/B23: A Multifunctional Chaperone in Ribosome Biogenesis and Chromatin Remodeling. Biochem. Res. Int., 195209, doi: 10.1155/2011/195209.

Lirussi L, Antoniali G, Vascotto C, D'Ambrosio C, Poletto M, Romanello M, Marasco D, Leone M, Quadrifoglio F, Bhakat KK, Scaloni A, Tell G. (2012) Nucleolar accumulation of APE1 depends on charged lysine residues that undergo acetylation upon genotoxic stress and modulate its BER activity in cells. Mol. Biol. Cell. 23, 4079- 4096, doi: 10.1091/mbc.E12-04-0299.

Ma HT, Poon RY. (2017) Synchronization of HeLa Cells. Methods Mol Biol 1524, 189-201, doi: 10.1007/978-1-4939-6603-5_12.

Maggi LB, Kuchenruether M, Dadey DYA, Schwope RM, Grisendi S, et al. (2008) Nucleophosmin serves as a rate limiting nuclear export chaperone for the mammalian ribosome. Mol Cel Biol 28, 7050-7065, doi: 10.1128/MCB.01548-07.

Maher RL, Bloom LB. (2007) Pre-steady-state kinetic characterization of the AP endonuclease activity of human AP endonuclease 1. J Biol Chem. 2007 282(42), 30577-30585, doi: 10.1074/jbc.M704341200.

Masuda Y, Bennett RA, Demple B (1998) Dynamics of the interaction of human apurinic endonuclease (Ape1) with its substrate and product. J. Biol. Chem. 273 (46), 30352-30359, doi: 10.1074/jbc.273.46.30352.

Mitrea DM, Cika JA, Stanley CB, Nourse A, Onuchic PL, Benerjee, PR, Phillips AH, Park C-G, Deniz AA, Kriwacki RW (2018) Self-interaction of NPM1 modulates multiple mechanisms of liquid-liquid phase separation. Nature Communications 9, 842, doi: 10.1038/s41467-018-03255-3.

Mol CD, Izumi T, Mitra S, Tainer JA (2000) DNA-bound structures and mutants reveal abasic DNA binding by APE1 and DNA repair coordination. Nature 403, 451-456, doi: 10.1038/35000249.

Moore HM, Bai B, Matilainen O, Colis L, Peltonen K, Laiho M. (2013) Proteasome activity influences UV-mediated subnuclear localization changes of NPM. PLoS One. 8(3), e59096, doi: 10.1371/journal.pone.0059096.

Ogawa LM, Baserga SJ. (2017) Crosstalk between the nucleolus and the DNA damage response. Mol Biosyst. 13(3):443-455, doi: 10.1039/c6mb00740f.

Okuwaki M, Matsumoto K, Tsujimoto M, Nagata K. (2001) Function of nucleophosmin/B23, a nucelolar acidic protein, as a histone chaperone. FEBS Lett. 506(3), 272-276.

Olazabal-Herrero A, García-Santisteban I, Rodríguez JA. (2016) Mutations in the “Fingers” subdomain of the deubiquitinase USP1 modulate its function and activity. FEBS J 283(5), 929-946, doi: 10.1111/febs.13648.

Parsons J.L. and Dianov G.L. (2013) Co-ordination of base excision repair and genome stability. DNA Repair 12, 326-333. doi: 10.1016/j.dnarep.2013.02.001

Pilié PG, Tang C, Mills GB, Yap TA. (2018) State-of-the-art strategies for targeting the DNA damage response in cancer. Nat Rev Clin Oncol. doi: 10.1038/s41571-018-0114-z.

Poletto M, Vascotto C, Scognamiglio PL, Lirussi L, Marasco D, Tell G. (2013) Role of the unstructured N-terminal domain of the hAPE1 (human apurinic/apyrimidinic endonuclease 1) in the modulation of its interaction with nucleic acids and NPM1 (nucleophosmin). Biochem J 452(3), 545-557, doi: 10.1042/BJ20121277.

Poletto M, Malfatti MC, Dorjsuren D, Scognamiglio PL, Marasco D, Vascotto C, Jadhav A, Maloney DJ, Wilson DM 3rd, Simeonov A, Tell G. (2016) Inhibitors of the apurinic/apyrimidinic endonuclease 1 (APE1)/nucleophosmin (NPM1) interaction that display anti-tumor properties. Mol Carcinog 55(5), 688-704, doi: 10.1002/mc.22313.

Scott D.D, and Oeffinger M. (2016) Nucleolin and nucleophosmin: nucleolar proteins with multiple functions in DNA repair. Biochem. Cell Biol. 94, 419-432, doi: 10.1139/bcb-2016-0068.

Sekhar KR, Reddy YT, Reddy PN, Crooks PA, Venkateswaran A, McDonald WH, Geng L, Sasi S, Van Der Waal RP, Roti JL, Salleng KJ, Rachakonda G, Freeman ML. (2011) The novel chemical entity YTR107 inhibits recruitment of nucleophosmin to sites of DNA damage, suppressing repair of DNA double-strand breaks and enhancing radiosensitization. Clin Cancer Res 17(20), 6490-6499, doi: 10.1158/1078-0432.CCR-11-1054.

Sharma SK, De Los Rios P., Christen P, Lustig A, Goloubinoff P. (2010) The kinetic parameters and energy cost of the Hsp70 chaperone as a polypeptide unfoldase. Nature Chem Biol, doi: 10.1038/nchembio.455.

Vascotto C, Fantini D, Romanello M, Cesaratto L, Deganuto M, Leonardi A, Radicella JP, Kelley MR, D'Ambrosio C, Scaloni A, Quadrifoglio F, Tell G. (2009) APE1/Ref-1 interacts with NPM1 within nucleoli and plays a role in the rRNA quality control process. Mol. Cell Biol. 29, 1834-1854, doi: 10.1128/MCB.01337-08.

Vascotto C, Lirussi L, Poletto M, Tiribelli M, Damiani D, Fabbro D, Damante G, Demple B, Colombo E, Tell G. (2014) Functional regulation of the apurinic/apyrimidinic endonuclease 1 by nucleophosmin: impact on tumor biology. Oncogene 33, 2876-2887, doi: 10.1038/onc.2013.251.

Vidal AE, Boiteux S, Hickson ID, Radicella J.P. (2001) XRCC1 coordinates the initial and late stages of DNA abasic site repair through protein-protein interactions. EMBO J.

20 (22), 6530-6539, doi: 10.1093/emboj/20.22.6530.

Vuzman D, Azia A, Levy Y. (2010) Searching DNA via a “monkey bar” mechanism: The significance of disordered tails. J. Mol. Biol. 396, 674-684, doi: 10.1016/j.jmb.2009.11.056.

Wang W, Budhu A, Forgues M, Wang XW (2005) Temporal and spatial control of nucleophosmin by the Ran-CRM1 complex in centrosome duplication. Nat Cell Biol 7, 823-830, doi: 10.1038/ncb1282.

Wilson DM 3rd, Simeonov A. (2010) Small molecule inhibitors DNA repair nuclease activities of APE1. Cell Mol Life Sci. 67(21), 3621-3631, doi: 10.1007/s00018-010-0488-2.

Yang K, Wang M, Zhao Y, Sun X, Yang Y, Li X, Zhou A, Chu H, Zhou H, Xu J, Wu M, Yang J, Yi J. (2016) A redox mechanism underlying nucleolar stress sensing by nucleophosmin. Nat. Commun. 7, 13599, doi: 10.1038/ncomms13599.

Yu E, Gaucher SP, Hadi MZ. (2010) Probing conformational changes in Ape1 during the progression of base excision repair. Biochemistry 49(18), 3786-3796, doi: 10.1021/bi901828t.

Ziv O, Zeisel A, Mirlas-Neisberg N, Swain U, Nevo R, Ben-Chetrit N, Martelli MP, Rossi R, Schiesser S, Canman CE, Carell T, Geacintov NE, Falini B, Domany E, Livneh Z. (2014) Identification of novel DNA-damage tolerance genes reveals regulation of translesion DNA synthesis by nucleophosmin. Nat Commun 5: 5437, doi: 10.1038/ncomms6437

Zou Y, Wu J, Giannone RJ, Boucher L, Du H, Huang Y, Johnson DK, Liu Y, Wang Y. (2008) Nucleophosmin/B23 negatively regulates GCN5-dependent histone acetylation and transactivation. J Biol Chem 283(9), 5728-5737, doi: 10.1074/jbc.M709932200.

Table 1: Thermodynamic parameters of the binding of APE1 to either wild type NPM1 or AML-related mutant A.

	K_D (μM)	n	ΔH (KJ/mol)	ΔS (J/mol·K)	ΔG (KJ/mol)
NPM1·APE1	13.3 ± 8.5	2.3 ± 0.8	9.6 ± 2.2	127.8 ± 8.8	-27.8 ± 1.9
NPM1mutA·APE1	12.5 ± 3.8	2.0 ± 0.9	9.2 ± 3.5	125.8 ± 13.0	-27.6 ± 0.8

Figure legends

Figure 1. Changes in APE1 and NPM1 localization upon $KBrO_3$ treatment. HeLa cells were co-transfected with APE1-mCherry and YFP-NPM1 and treated, after 24 h, with 300 mM $KBrO_3$ (or left untreated). After recovering in fresh medium for 3 h, soluble proteins were extracted with CSK buffer containing Triton X-100 prior to fixation. Whereas in normal conditions (untreated), APE1 is lost, and NPM1 remains almost exclusively in nucleoli, in treated cells, APE1 becomes "immobilized", as previously described (Campalans et al., 2013), and NPM1 partly exits the nucleolus, remaining fixed on regions through nucleoplasm. Scale bar corresponds to 5 μm.

Figure 2. (A) NPM1p199 is excluded from nucleoli. Endogenous NPM1 and NPM1p199 are detected by immunostaining (red). Nuclei are shown in blue. Scale bar, 10 μm. **(B, C) Under oxidative conditions, the amount of NPM1p199 increases to a level comparable to mitosis.** HeLa cells were treated with neocarzinostatin (NCS, 4h), $KBrO_3$ (0-300 mM, 30 min followed by 3 h recovery), nocodazole (Noco, 24h), or left untreated (UT). Then, cell extracts were migrated in 12.5 % PAGE, blotted, and the membrane exposed to anti-NPM1p199 and anti-NPM1; GAPDH and tubulin were~~as~~ used as load control. **(D)** Relative intensities~~-~~of the Western blot bands corresponding to NPM1p199 and NPM1 as a function of $KBrO_3$ concentration.
Both values were normalized against tubulin as load control. For comparison, the signal corresponding to the treatment with nocodazole is also shown. Data are averages of two experiments, bars indicating standard error. Asterisks mean statistically significant differences ($p < 0.05$) with respect to the control.

Figure 3. NPM1 and APE1 form a defined, saturable complex where several molecules of APE1 bind to the NPM1 pentamer. (A) Native 4-16% polyacrylamide gel of mixtures of 0.1 μM NPM1 (pentamer) and 0-10 μM APE1. **(B)** Mixtures of 1 μM NPM1 (pentamer) and 0-100 μM APE1. **(C,D)** Binding curves based on densitometry of the band corresponding to the complex in experiments with 0.1 μM (C) and 1 μM NPM1 (D). Data are averages from 3-5 experiments.

Figure 4. APE1/NPM1 binding as followed by ITC. Binding isotherm obtained upon injection of APE1 (400 μM) onto NPM1 (10.8 μM), at 20ºC and the fit to a model of n independent sites. Insert: baseline-corrected instrumental response.

Figure 5. Comparison of APE1 binding by wild type NPM1, NPM1MutA, NPM1ΔC106 and NPM1 core. (A) Binding curves based on native electrophoresis assays with 0.5 μM (NPM1core) or 0.1 μM pentamer (for the rest of NPM1 variants). The corresponding fittings to a simple binding model are also shown, with indication of the estimated K_D values. **(B)** Comparison of NPM1 binding by wild type APE1 and APE1ΔN33.

Figure 6. (A) Binding to magnesium and/or abasic DNA conformationally stabilizes APE1. Thermal scans based on ellipticity at 222 nm of 4 μM apo APE1 (0.5 mM EDTA) (black), holo APE1 (5 mM $MgCl_2$) (red), apo APE1 in the presence of equimolar amount of oligonuleotide "Dumbbell P" (dark blue) and holo APE1 plus DNA (green). Scans were corrected for the DNA contribution. The heating rate was 1ºC/min. **(B) Secondary structure of APE1 and APE1ΔN33 is sensitive to DNA binding.** Amide I band of the infrared spectra of APE1 (solid line) and APE1ΔN33 (broken line) in the absence (blue) and presence (red) of equimolar amounts of the oligo "Dumbbell P". The spectra were recorded in D_2O buffer at 20ºC. The contribution of buffer was substracted and the baseline was corrected between 1700 and 1600 cm^{-1}.

Figure 7. NPM1 stimulates APE1 catalyzed incision of abasic DNA, and favors specific binding of APE1 to the substrate. (A) Incision of an abasic- mimicking oligonucleotide (5 μM) by increasing concentrations of APE1 as followed by DNA urea-polyacrylamide denaturing electrophoresis, in the absence (empty symbols) and in the presence (solid symbols) of 5 μM NPM1. **(B)** Binding of 0 – 10 μM APE1 to 10 nM Dumbbell S in the absence (empty) or presence (solid) of 5 μM NPM1, based on fluorescence anisotropy. **(C)** The same binding data of panel B shown in the range 0-1 μM APE1 and logarithmic scale and with the corresponding fitted curves (p- value < 0.05). Data are averages of three experiments, bars indicating standard deviation.

Figure 8. Effect of NPM1 on APE1/DNA complex formation as followed by native electrophoresis. (A) Native 4-16% PA gel of mixtures of 5 μM oligo (O), 2 μM APE1 (A) and 0-10 μM NPM1 (N) (pentamer), along with the corresponding individual species and binary mixtures as controls. The lanes corresponding to the ternary mixtures are labelled according to NPM1 concentration. Images of the gel stained with Coomassie for detection of proteins (blue) and GelRed for DNA (white) are overlaid. **(B)** Native PAGE of a mixture of 5 μM oligo and 20 μM APE1 in the absence (OA) and

in the presence (OAN) of 1 μM NPM1. The gel was stained as in (A). **(C)** Densitometry of the band corresponding to the APE1:DNA (1:1) complex stained with Coomassie (squares) or GelRed (triangles) as a function of NPM1 concentration.

Fig. 1

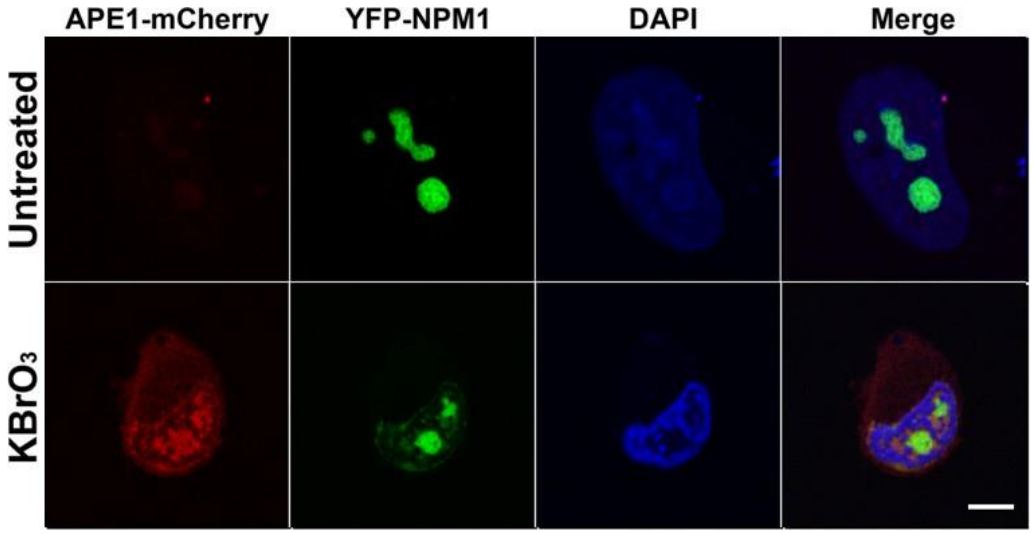

Fig. 2

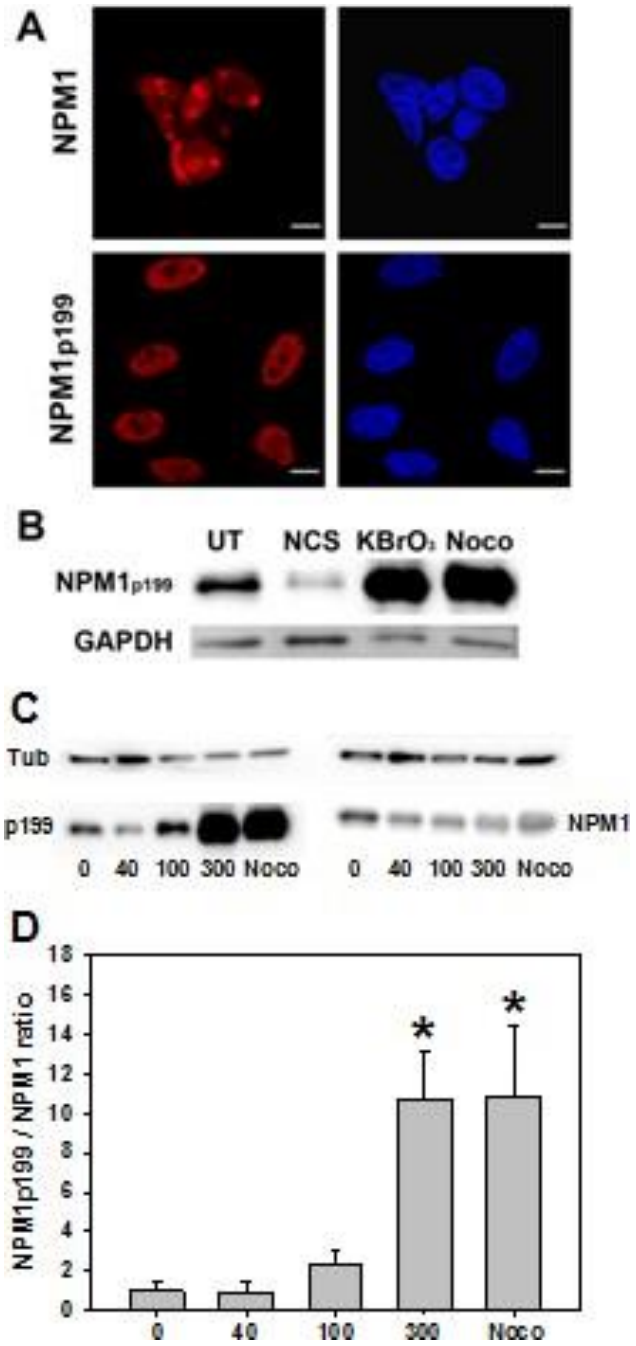
A
NPM1
NPM1p199
B
UT
NCS
KBrO3
Noco
NPM1p199
GAPDH
C
Tub
p199
NPM1
0 40 100 300 Noco
0 40 100 300 Noco
D
NPM1p199 / NPM1 ratio
0
2
4
6
8
10
12
14
16
18
*
*
0
40
100
300
Noco

Fig. 3

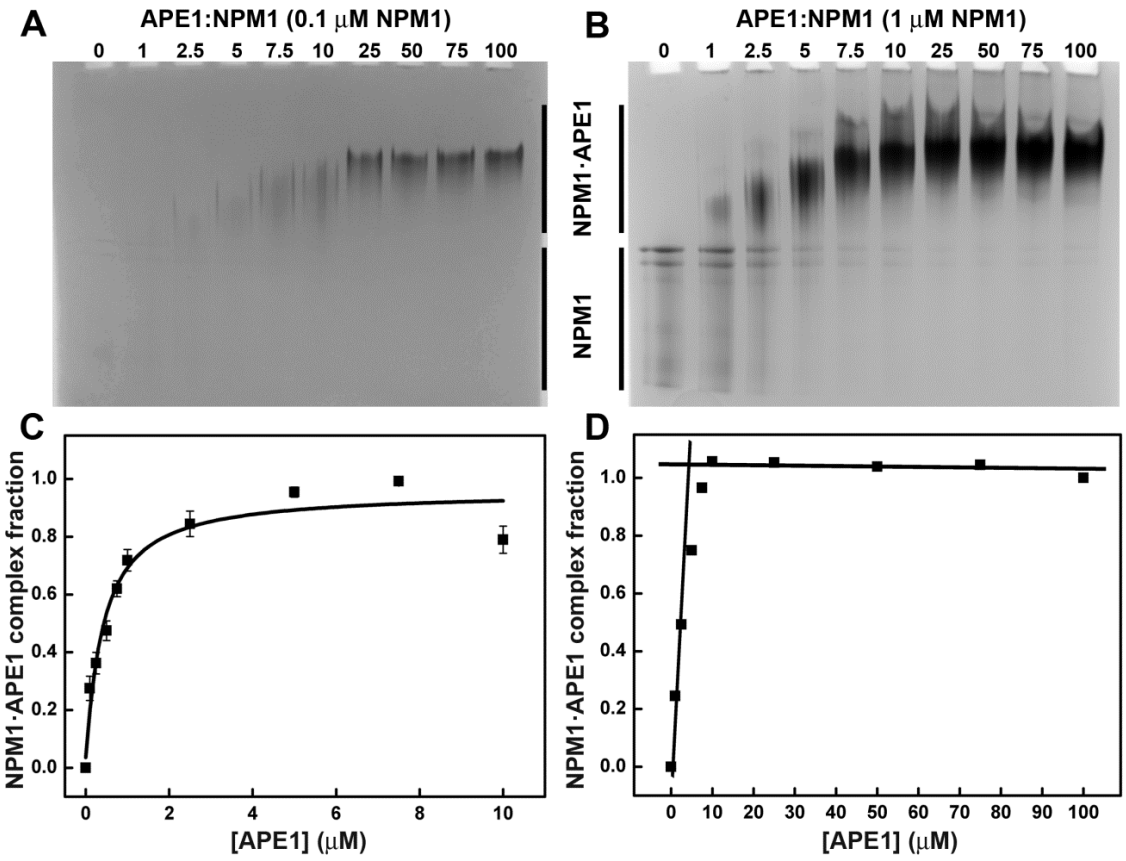
A
APE1:NPM1 (0.1 μM NPM1)
0 1 2.5 5 7.5 10 25 50 75 100
B
APE1:NPM1 (1 μM NPM1)
0 1 2.5 5 7.5 10 25 50 75 100
NPM1·APE1
NPM1
C
NPM1·APE1 complex fraction
[APE1] (μM)
D
NPM1·APE1 complex fraction
[APE1] (μM)

Fig. 4.

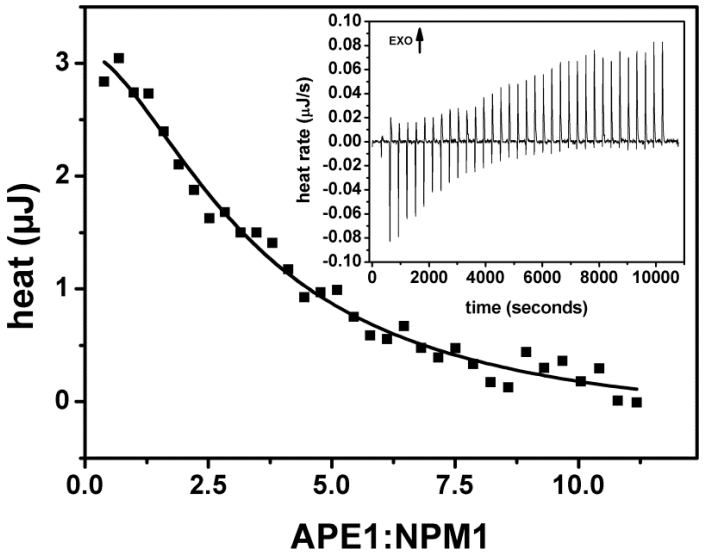

Fig. 5.

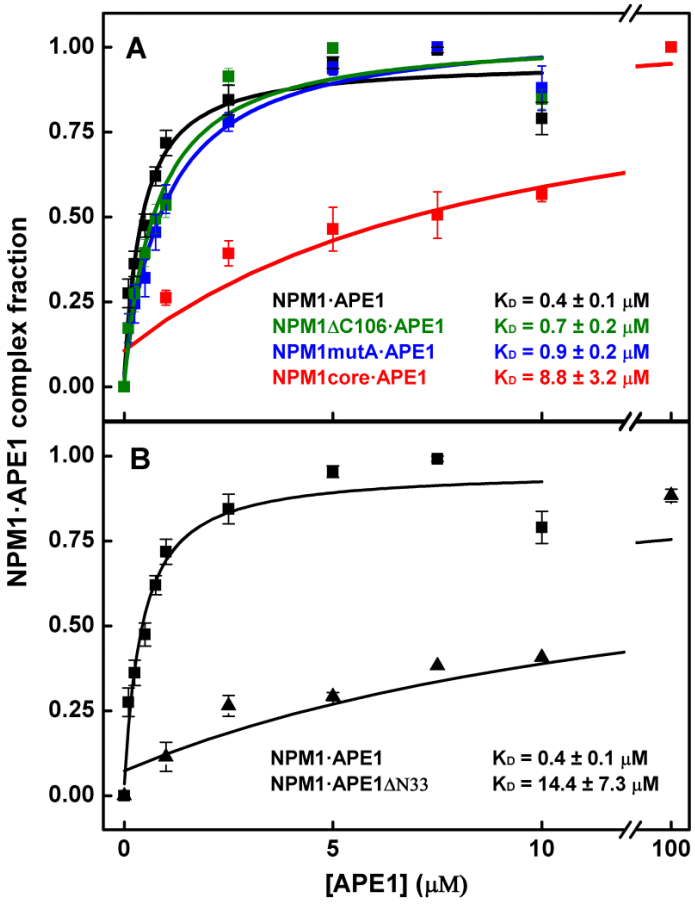
A
B
NPM1·APE1 complex fraction
1.00
0.75
0.50
0.25
0.00
NPM1·APE1
NPM1ΔC106·APE1
NPM1mutA·APE1
NPM1core·APE1
KD = 0.4 ± 0.1 μM
KD = 0.7 ± 0.2 μM
KD = 0.9 ± 0.2 μM
KD = 8.8 ± 3.2 μM
NPM1·APE1
NPM1·APE1ΔN33
KD = 0.4 ± 0.1 μM
KD = 14.4 ± 7.3 μM
0
5
10
100
[APE1] (μM)

Fig. 6

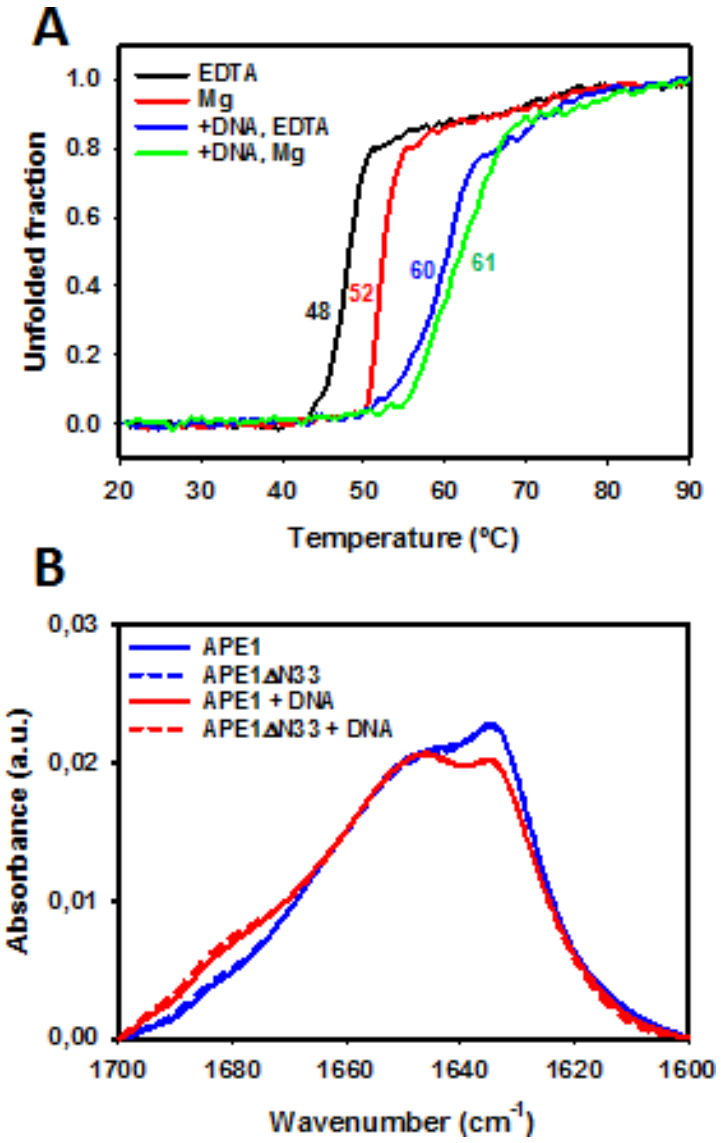
A
EDTA
Mg
+DNA, EDTA
+DNA, Mg
Unfolded fraction
1.0
0.8
0.6
0.4
0.2
0.0
48
52
60
61
20
30
40
50
60
70
80
90
Temperature (°C)
B
APE1
APE1ΔN33
APE1 + DNA
APE1ΔN33 + DNA
Absorbance (a.u.)
0,03
0,02
0,01
0,00
1700
1680
1660
1640
1620
1600
Wavenumber (cm-1)

Fig. 7

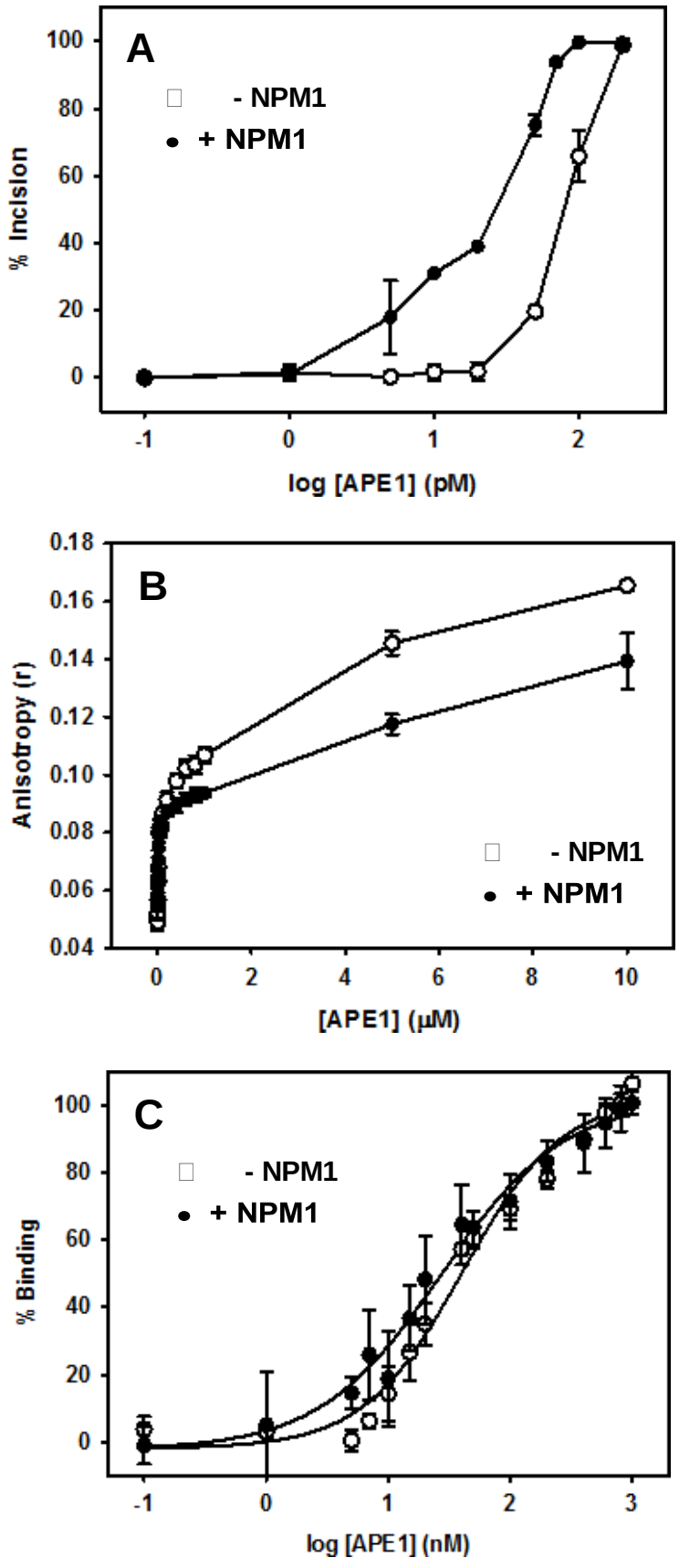
A
- NPM1
+ NPM1
% Incision
log [APE1] (pM)
B
- NPM1
+ NPM1
Anisotropy (r)
[APE1] (μM)
C
- NPM1
+ NPM1
% Binding
log [APE1] (nM)

Fig. 8

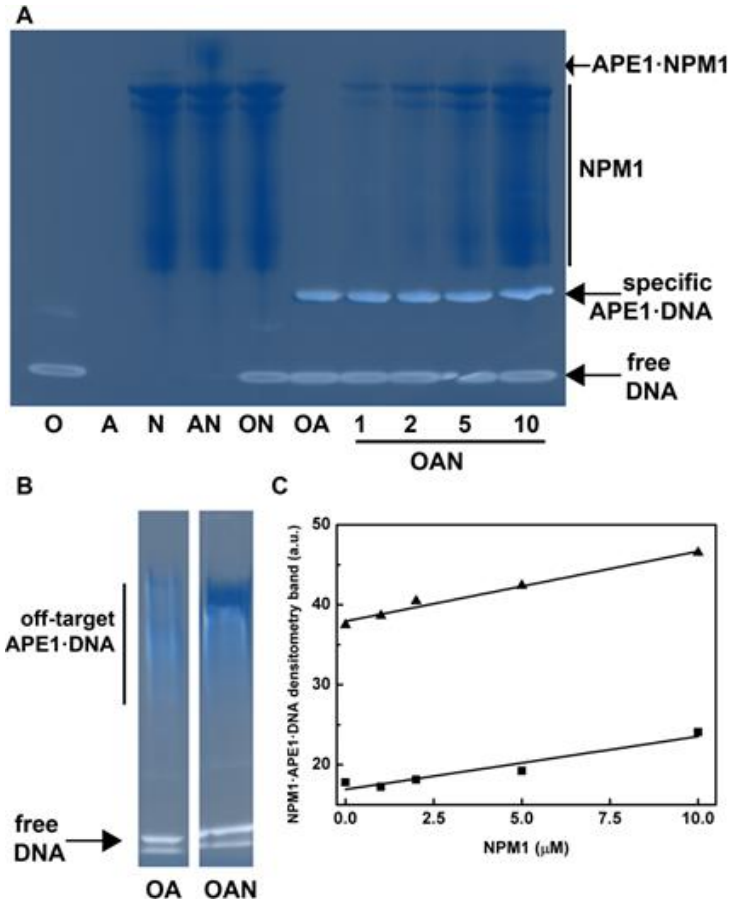
A
APE1·NPM1
NPM1
specific
APE1·DNA
free
DNA
O A N AN ON OA 1 2 5 10
OAN
B
off-target
APE1·DNA
free
DNA
OA OAN
C
NPM1-APE1-DNA densitometry band (a.u.)
50
40
30
20
0.0
2.5
5.0
7.5
10.0
NPM1 (μM)